Electron-phonon coupling in perovskites studied by Raman Scattering

V G Sathe[1], **S Tyagi and G Sharma**

UGC-DAE Consortium for Scientific Research
University Campus, Khandwa Road, Indore, M.P. INDIA

E-mail: vasant@csr.res.in

Abstract. Raman scattering is an unique technique for characterization and quantification of electron-phonon, spin-phonon and spin-lattice coupling in many of the currently prominent compounds like multiferroics and manganites. In manganites, it is understood now that a phase separated landscape with coexisting metallic and insulating regions exist in most of the compounds and application of small external perturbation causes an alteration in this landscape. In such scenario, local metallic regions grow suddenly at the expense of insulating regions below the magnetic ordering temperature. Such regions can be characterized effectively using Raman scattering measurements where delocalized electrons couple with the adjacent phonon peaks giving a Fano resonance in the form of asymmetric line shape.

1. Introduction

Perovskites, currently are the hot topic of research as they show very fascinating properties like, superconductivity, colossal magneto-resistance, colossal dielectric properties, multiferroic behaviour and thus results in a wide variety of applications. Raman spectroscopy is an ideal tool to detect electron-phonon coupling, spin-phonon coupling and spin-lattice coupling and therefore has been extensively used in detecting above phenomena in perovskites. In this paper, examples of electron-phonon coupling detected by Raman spectroscopy in metallic $LaMnO_{3+\delta}$ films is described.

Manganites show very strong coupling between the charge carriers, the localized spin moments of the manganese ions and the lattice structure. Such a coupling is manifested in the structural modification on application of magnetic field [1]. The main cause of such a structural modification is attributed to the changes in tolerance factor of the perovskite structure [2]. The tolerance factor gives a measure of Mn-O-Mn bond angle deviation from 180°. For example, the deviation is larger in orthorhombic structure leading to charge localization than compared to rhombohedral lattice where charges are de-localized. In such a way, the lattice degree of freedom is coupled with the kinetic energy of the conduction e_g electrons and holes. To understand the mechanisms of the colossal magnetoresistance, many attempts were made taking into account the strong interplay of magnetism, electron-lattice coupling, and orbital and charge ordering in these materials. It was shown earlier that double exchange alone cannot explain the large magneto-resistance in these materials [3]. Present understanding about the phenomena revolves around a phase separation scenario, [4, 5, 6, 7] the collapse of a phase coexisting and competing with other phases, into an energetically more favourable

state that is triggered by either temperature or an external stimuli like magnetic field, electric field, etc. [8]. The insulator-metal transition induced by small perturbations like magnetic field [9], x-rays [10], visible photons [11, 12], current [13] and even acoustic pulses [14] signifies that the system is electronically phase separated. A large number of mechanisms of matching energies are simultaneously active in the system, involving strong correlations among lattice and electronic degrees of freedom.

$LaMnO_{3\pm\delta}$ compounds show range of oxygen nonstoichiometry [15]. The oxygen excess 'δ', produces La and Mn vacancies, because of the trouble in accommodating excess oxygen atoms interstitially in the closed packed perovskite structure [16]. The excess oxygen produces Mn^{4+} ions along with Mn^{3+} ions in the system. It is known that the presence of Mn^{4+} is accompanied with the decrease in degree of distortion of oxygen octahedra leading to structural alteration [16]. Also Mn^{4+} transforms the system to ferromagnetic-metallic state. Therefore, the Mn-vacancies are likely to be more efficient for the electronic delocalization than the substitution on the La site. The Mn-vacancies leads to a randomization of the magnetic interaction and this inhomogeneous magnetic state is related to the local structural distortion. It is shown earlier that the local lattice distortion is highly coupled with the magnetic order and a less distorted pseudo cubic structure supports ferromagnetic ordering and metal-like conductivity [17]. A direct correlation between Raman mode intensities induced due to Jahn-Teller distortion and metallic-like conductivity is observed in $LaMnO_{3+\delta}$ films [18]. Therefore in these compounds, there should be a possibility of co-existing continuum scattering due to metallic regions along with phononic scattering. In many cases, these electronic and phononic scattering processes interacts strongly leading to Fano line shape. "Fano resonance" effect is reported previously in many compounds due to onset of metallicity in the system [19, 20, 21].

In this report we show strong electron-phonon coupling in conducting $LaMnO_{3+\delta}$ films reflected in the form of Fano asymmetric line shape in one of the Raman modes.

2. Experimental:

The parent $LaMnO_3$ (LMO) bulk compound was prepared by using standard solid-state reaction method by taking the stoichiometric amount of precursors having 99.99 % from Aldrich. $LaMnO_{3+\delta}$ films were deposited epitaxially on $LaAlO_3$ (LAO) (001) substrate using pulsed laser deposition technique equipped with an excimer laser λ = 248 nm. During the preparation, the substrate temperature was kept at ~650°C. All the films were prepared in 250 mTorr oxygen pressure. After deposition the films were annealed for 30 minutes in-situ at ~650°C in different oxygen environments 150 mTorr, 450 mTorr, 1000 mTorr and 1 atmosphere (atm) respectively and then the heater was slowly cooled down to room temperature. The thickness of all the films was kept at ~200 nm. After deposition the films were characterized by X-Ray diffraction (XRD) technique using a Rigaku make powder diffractometer fitted on a rotating anode (18 KW) X-Ray generator with Cu target. Resistivity of the films was measured using standard four-probe method. Raman spectra were collected in backscattering geometry using a Ar^+ excitation source (λ=488 nm) coupled with a Labram-HR800 micro Raman spectrometer equipped with a ×50 objective, appropriate notch filter and peltier cooled charge coupled device detector. For the low temperature Raman measurements, the sample was mounted on a THMS600 stage from Linkam UK, with temperature stability of ±0.1 K.

3. Results and discussions:

The x-ray diffraction of the films are shown in figure 1. The pattern around (002) pseudo cubic unit cell is only shown for better comparison. The peaks showed a regular trend, the 2θ value shows an increase with increasing oxygen content (δ) in the film. Larger 2θ value means shorter out of plane lattice parameter which in turn signifies larger in plane lattice parameter. This indicates that the film relaxes with increasing oxygen content. Generally, relaxation process leads to *strain disorder* [4,5] which supports phase separation.

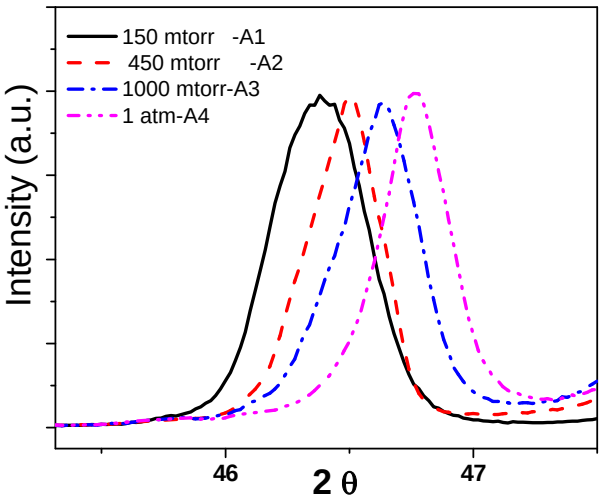

Figure 1: X-ray diffraction of films collected with Cu Kα radiation. The diffraction pattern is normalized and only region around (002) (pseudo-cubic) peak of LaMnO3 is shown.

The resistivity of all the film as a function of temperature is shown in figure 2. It can be seen that film A1 and A2 are insulating with small kink showing a hint to the presence of insulator to metal transition at 186 K. On the other hand film A3 and A4 show a clear insulator to metal transition around 206 K and 270 K respectively. From the resistivity data it can be concluded that all the films are phase separated with predominant insulating phase fraction in the films A1 and A2, dominant metallic fraction in the film A3 and mostly metallic fraction in the film A4.

Figure 3 shows the doping dependence of Raman spectra of $LaMnO_{3+\delta}$ films with increasing δ (A1 – A4) in parallel (XX) polarization at 280 K and 240 K respectively.

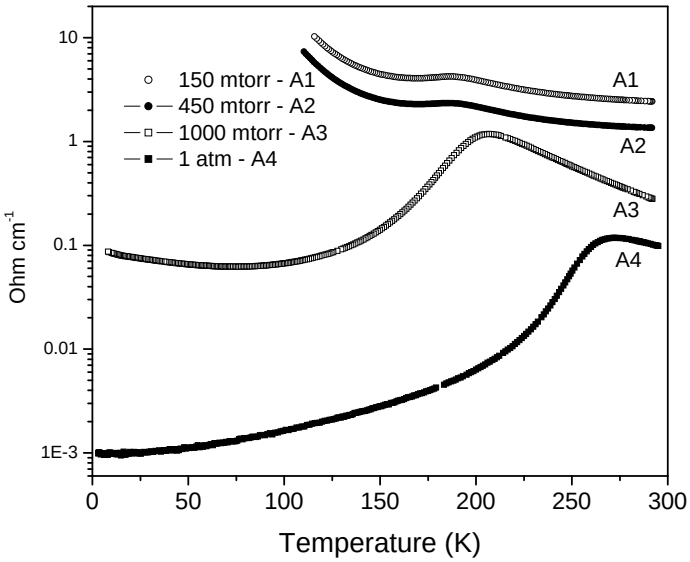

Figure 2: Resistivity as a function of temperature for the $LaMnO_{3+\delta}$ films with different oxygen doping.

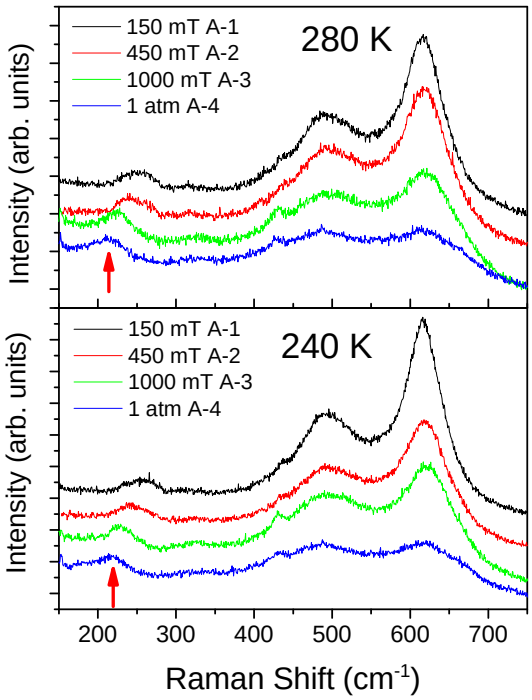

Figure 3: Comparison of Raman spectra for the films A-1, A-2, A-3, and A-4 collected at 280 K and at 240 k. The spectra are shifted vertically for clarity. The arrow marks the peak showing asymmetric line shape.

The Raman peaks around 490 cm^{-1} and 620 cm^{-1} shows behaviour typical of a metallic and insulating phases and are discussed in ref. [18] and will not be a part of discussion in this paper. The low frequency peaks between 200 and 300 cm^{-1} shows an interesting trend and that will be the focus of this report. The Raman spectra in this region for insulating samples i.e. the samples A-1 and A-2 are significantly different than for the metallic samples A-3 and A-4. The peak in insulating sample is broad, probably resulting from a combination of two peaks. It falls at 250 cm^{-1} and 270 cm^{-1} that is typical of an orthorhombic structure. In A-3, the peaks shifts to lower frequency around 225 cm^{-1} and is sharper when compared with the samples A-1 and A-2. This peak further shifts to 215 cm^{-1} for the mostly metallic sample A-4. Such a peak shift clearly suggests that all the samples are phase separated with mixture of orthorhombic and rhombohedral structures. The red shift and sharpening of the peak in Raman spectra of mostly metallic (A-4) film also suggests that the oxygen doping is reducing the tilt angle of the MnO_6 octahedra along y-axis, making it rhombhohedral [22]. According to ref. [22] this mode in the metallic sample is assigned to in-phase rotational vibration of the MnO_6 octahedra about the y-axis with A_g character while the same mode in the insulating sample is assigned to out-of-plane rotational of the MnO_6 octahedra around the x-axis. This shows that the tilt angle of the MnO_6 octahedra decreases significantly with increasing oxygen doping.

The most important result which is the focus of this report is the asymmetric peak shape of the A_g mode (~215 cm^{-1}) observed only for dominant metallic (A-3 and A-4) samples. The Raman spectra collected at 160 K, 120 K, and 80 K for the four films is compared in figure 4. It can be noticed that the asymmetry in A_g mode is absent for the samples A-1 and A-2 while it is more for A-4 compared to A-3. The Raman intensity falls significantly after this Raman mode and the electronic background remains suppressed after this peak. This clearly indicates the presence of strong interaction between electronic background and the phonon modes. Observation of this phenomenon only in the samples with metallic character further strengthens this argument.

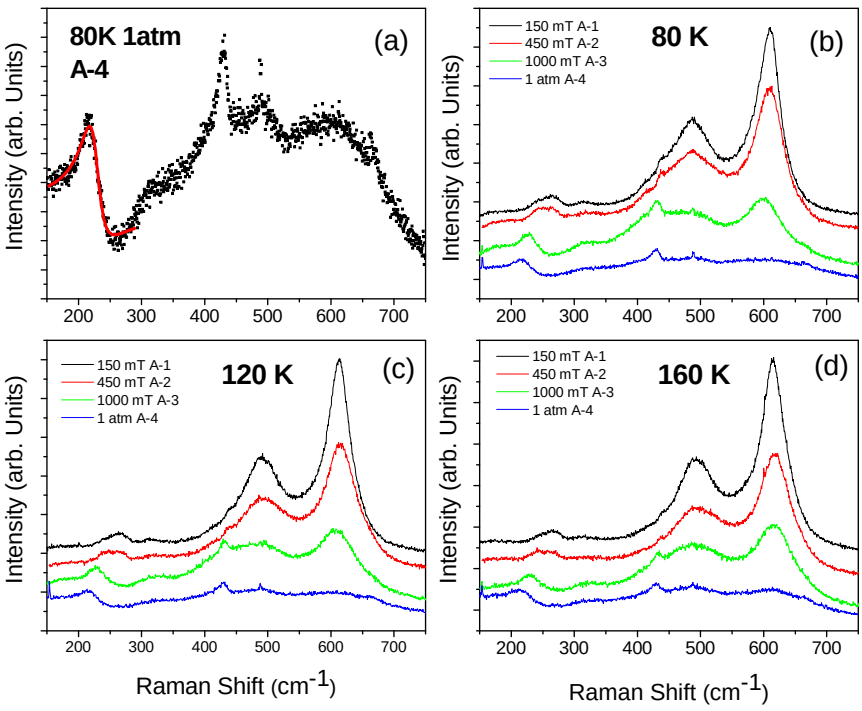

Figure 4: (a) The Fano line shape fit to the assymetric peak ~215 cm-1 of sample A-4 collected at 80K. The dots represent experimental points while the line represents fit to the data using Fano line shape. Comparison of Raman spectra for the films A-1, A-2, A-3, and A-4 collected at 80 K (b), at 120 k (c), and at 160 k (d). The spectra are shifted vertically for clarity.

The peak shape has been fitted with Fano function:

$$I(\omega) = I_C \frac{|q+\varepsilon|^2}{1+\varepsilon^2} + I_b(\omega),$$

and is shown in figure 4 (a). Here q is the asymmetry parameter, $\varepsilon = (\omega - \omega_p)/\Gamma$, ω_p is renormalized phonon frequency, and Γ is the line width. As the peak becomes more asymmetric with decreasing temperature, 'q' decreases. The inverse of the asymmetry parameter (1/q) is a measure of metallicity in the system [23]. It is observed that the Fano parameter increases as the temperature is decreased for both A-3 and A-4. When compared, the asymmetry parameter is higher for A-4 from that for A-3 at all the temperatures. The asymmetry parameter (q) deduced from the Fano profile fit of $A_g(1)$ mode as a function of temperature is plotted for both the films in Figure 5 (a,b), here the solid line is guide to the eye.

A decrease in the parameter *q* with increasing temperature is observed for both the compounds signifying enhancement of metallicity in this phase separated system with decreasing temperature. Such an increment of asymmetry in Fano line shape of Raman mode was reported in Mott-Hubbard insulating titanates where asymmetry evolves from insulating $GdTiO_3$ and become maximum for nearly metallic $LaTiO_3$ [24]. In the present system, the asymmetry parameter *q* shows a sudden change below ferromagnetic transition temperature (see Figure 5) establishing the connection between electron-phonon coupling and the spin degree of freedom.

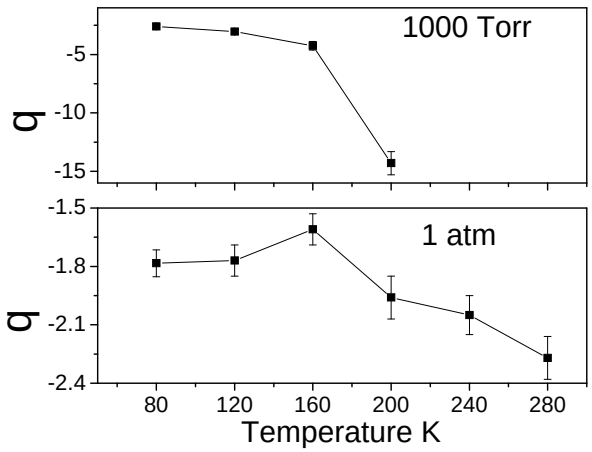

Figure 5: The Fano resonance parameter "*q*" obtained from fitting the Ag mode in films A-3 and A-4 at various temperatures.

4. Summary:

In summary; Raman spectroscopic studies as a function of temperature have been carried out on $LaMnO_{3+\delta}$ films. Evidence of Fano resonance certifying coupling between discrete phonon modes and electronically originated continuum has been observed signifying the presence of strong electron-phonon coupling. The existence of Fano line shape in only metallic films establishes phase separated metallic and insulating regions as predicted due to charge and orbital order/disorder transition in this system. Temperature dependence of asymmetry parameter derived from Fano profile reaffirms the development of the metallic region with ferromagnetic order in the metallic films.

References:

[1] Asamitau A, Moritomo Y, Tomioka Y, Arima T and Tokura Y 1995 *Nature* **373**, 407
[2] Rini M, Tobey R, Dean N, Itatani J, Tomioka Y, Tokura Y, Schoenlein R W & Cavalleri A 2007 *Nature* **449** 72
[3] Millis A J, Littlewood P B and Shraiman B I 1995 *Phys. Rev. Lett.* **74**, 5144
[4] Mishra D K, Sathe V G, Rawat R, Ganesan V, Kumar R, Sharma T K 2015 *Appl. Phys. Lett.* **106**, 072401
[5] Mishra D K, Sathe V G, Rawat R and Ganesan V 2013 *J. Phys.: Condens. Matter* **25** 175003
[6] Rawat R, Kushwaha P, Mishra D K, and Sathe V G 2013 *Phys. Rev. B* **87** 064412
[7] Mathur N and Littlewood P 2003 *Phys. Today* **56** 25
[8] Dagotto E Science 2005 **309** 257
[9] Campbell A J, Balakrishnan G, Lees M R and McKPaul D and McIntyre G J 1997 *Phys. Rev. B* **55** R8622
[10] Kiryukhin V, Casa D, Hill J H, Keimer B, Vigliante A, Tomioka Y & Tokura Y, 1997 *Nature* **386** 813
[11] Fiebig M, Miyano K, Tomioka Y and Tokura Y 1998 *Science* **280** 1925
[12] Miyano K, Tanaka T, Tomioka Y and Tokura Y 1997 *Phys. Rev. Lett.* **78** 4257
[13] Asamitsu A, Tomioka Y, Kuwahara H and Tokura Y 1997 *Nature* **388** 50
[14] Prabhakaran D, Coldea A I, Boothroyd AT and Blundell S J 2002 *J. Crystal Growth* **237-239** 806
[15] Tofield B C and Scott W R 1974 *J. Solid state Chem.* **10** 183
[16] Subias G, Garcia J, Blasco J, and Proietti M G 1998 *Phys. Rev. B.* **58**, 9287

[17] Dubey A and Sathe V G 2007 *J. Phys.: Condens. Matter* **19** 346232
[18] Dubey A, Sathe V G and Rawat R 2008 *J. Appl. Phys.* **104** 113530
[19] Baldini M, Struzhkin V V, Goncharov A F, Postorino P, and Mao W L 2011 *Phys. Rev. Lett.* **106**, 066402
[20] Marrocchelli D, Postorino P, Di Castro D, Arcangeletti E, Dore P, Cestelli Guidi M, Ray S and Sarma D D 2005 *Phys. Rev. B* **76**, 102405
[21] Mishra D K and Sathe V G 2012 *J. Phys.: Condens. Matter* **24** 252202
[22] Iliev M N and Abrashev M V 1998 *Phys. Rev.* B **57** 2872
[23] Fano U 1961 *Phys. Rev.* **124** 1866; Hartinger Ch, Mayr F, Loidl A and Kopp T 2004 *Phys. Rev. B* **70** 134415
[24] Reedyk M, Crandles D A, and Cardona M 1997 *Phys. Rev. B* **55** 1442